# Numerical Analyses on Wall Deflections and Ground Surface Settlements in Excavations

L W Wong*

SMEC Asia Limited, Hong Kong, China

*Corresponding author
doi: https://doi.org/10.21467/proceedings.133.42

**ABSTRACT**

Ground movements may cause damages to structures. Accurate estimations of ground movements are therefore essential for the risk assessment programs for projects involving underground constructions. Presented herein is a study on the influence of various parameters on the magnitudes and the distributions of ground movements during deep excavations with emphasis on the shapes of settlement troughs. Two-dimensional finite element analyses were conducted on 5 cases for the east end of Xiaonanmen Station in Taipei Metro. The hardening soil with small-strain stiffness was adopted to simulate the nonlinear stress-strain relationship of soils. The results indicate that the shapes of the settlement troughs are primarily affected by the depths of excavations and are relatively insensitive to the width of excavation or the thickness of the retaining wall. Based on the results obtained, the relationship between the width of the influence zone of settlement and the depth of excavation is established.

**Keywords:** Excavation, Hardening Soil Model, Small Strain, Settlement Trough, Influence Zone

## 1 Introduction

Xiaonanmen Station of Taipei Metro was constructed by using the bottom-up cut-and-cover method of construction. Adjoining the east end of the station is a 397 m long crossover tunnel with the depths of excavations increasing from 16.5 m to 21.7 m and widths of excavation reducing from 19.2 m to 8 m. This section of the route is ideal for the evaluation of the influences of the width and the depth of the pit on ground movements induced by excavation because there are only a few low-rise structures in the vicinity of the excavation with one-level basements under some of them. This drastically reduces the complexity of the problem. The 2-Dimensional analyses will be appropriate for back analyses on the ground movements.

This section of the tunnel route was previously studied with emphasis on the effectiveness of the 3 cross-walls in reducing the lateral deflections of the diaphragm walls located in close proximity to Lizhengmen, which is the South Gate of the City of Taipei and is now a historical heritage to be preserved (Wong and Hwang, 2021). Therefore, most of the soil and structural parameters adopted in the current study have previously been verified by matching the computed wall deflections with the observed wall deflections. The study presented herein is in fact an extension of this previous study with emphasis on ground settlements induced.

## 2 Case Studied

As depicted in Figure 1, at the junction of Xiaonanmem Station and the crossover tunnel, ground movements were monitored by 6 inclinometers, i.e., SID-2 to SID-4 and SID-6 to SID-8, embedded in the diaphragm walls. There were 20 settlement markers installed along Chongqin South Road, 6 piezometers installed at various depths outside the pit, and 7 piezometers inside the pit for monitoring the groundwater levels.



Proceedings DOI: 10.21467/proceedings.133; Series: AIJR Proceedings; ISSN: 2582-3922; ISBN: 978-81-957605-1-0

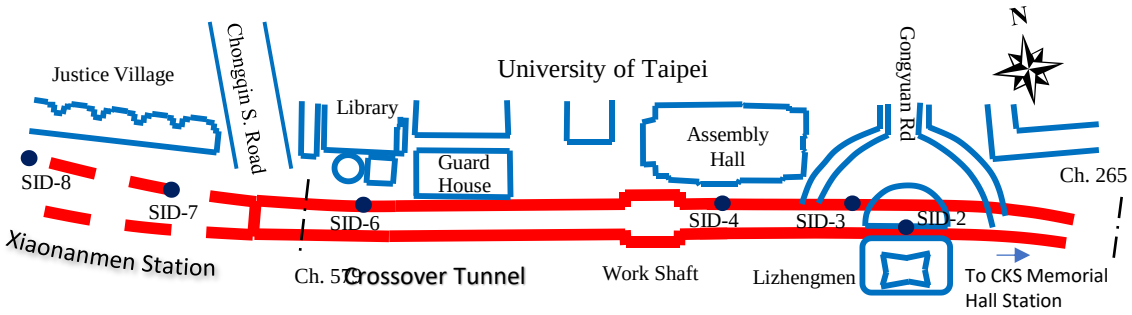


**Figure 1:** The crossover tunnel between Xiaonanmen Station and Chiang Kai Shek Memorial Hall Station

A representative excavation model is shown in Figure 2. The excavation was carried out to a depth of 16.5 m in 6 stages. The pit was retained by diaphragm walls of 0.8 in thickness and 31.5 m in length and was propped by steel struts at 5 levels. However, analyses were conducted to a depth of 23.5 m by adding 3 more stages to test the stability of the excavation if the excavation were continued.

## 2.1 Ground Condition

This section of the route is located in the T2 Geological Zone (MAA 1987) in the central Taipei Basin. As depicted in the soil profile shown in Figure 2, the Songshan Formation at the surface comprises six alternating sand (SM) and clay (CL) layers. Sublayers I, III, and V are sandy soils, and Sublayers II, IV, and VI are clayey soils. The properties of the six sublayers in the Songshan Formation have been well discussed in literatures (Moh and Ou 1979; MAA 1987). Underlying the Songshan Formation is a water-rich gravelly (GM) stratum, i.e., the so-called Jingmei Formation, which is a competent formation with very high stiffness and is frequently assumed to be the base of the numerical models. However, the base of the finite element model in this study is placed at a depth of 61 m to include a 15 m layer of the Jingmei Formation to ensure that the contribution of this formation to ground movement is accounted for.

The piezometric levels in the Jingmei Formation were lowered to a level near the bottom of the Songshan Formation in the 1970s due to excessive extraction of groundwater to supply water to the city, leading to significant reductions in water pressures in the Songshan Formation and substantial ground settlements as a result. The piezometric levels in the Jingmei Formation did not recover till the mid-1970s although pumping had been banned since 1968. The subsoils in the Songshan Formation in the central city area are thus substantially over-consolidated. This is particularly true for the clayey Sublayer II because the underlying sandy Sublayer I is so permeable that the piezometric level in Sublayer I essentially dropped by the same magnitudes as those in the Jingmei Formation

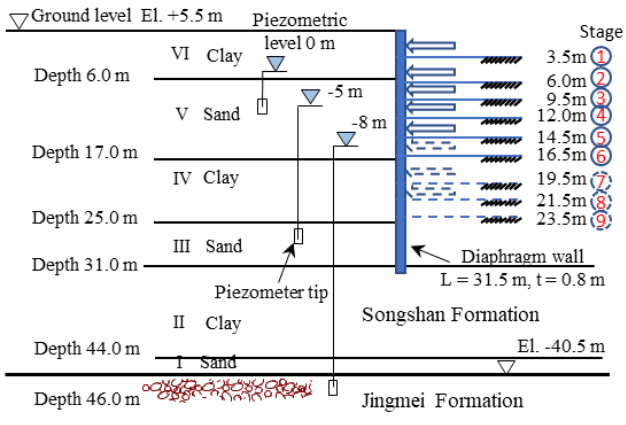


Note: Refer to Table 1 for width of excavation and thickness of diaphragm wall.

**Figure 2:** Soil profile of the Cross-over tunnel and excavation scheme

An advanced study was conducted by Geotechnical Engineering Specialty Consultant engaged by the Department of Rapid Transit Systems of Taipei City Government in the very early stage of the metro construction. This Designated Task studied the characteristics of the soils in the Taipei basin to provide the basic information required for the design and construction of metro facilities (Chin et al. 1994; Chin and Liu 1997). This was a research project so it was carried out under stringent supervision. Soil samples of high quality were obtained and tested with great care. The test results are therefore more reliable than those normally obtained. Hwang et al. (2013) summarized the results of the study and suggested that Figure 3 be adopted for estimating the undrained shear strengths of the clays in the T2 Zone.

The piezometric levels recorded by piezometers outside the pit are presented in Figure 2 and Figure 4. The drawdowns were small and, presumably, would not have a significant influence on wall deflections or ground settlements. Inside the pit, the groundwater table was maintained at a depth of 1m below the bottom of the excavation as the excavation proceeded.

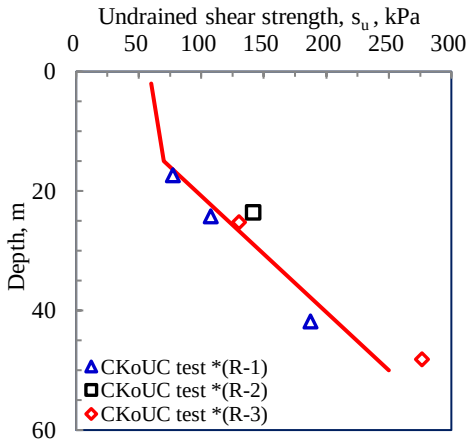


**Figure 3:** Estimated undrained shear strengths of clays in T2, TK2, and K1 Zones (Hwang et al. 2013)

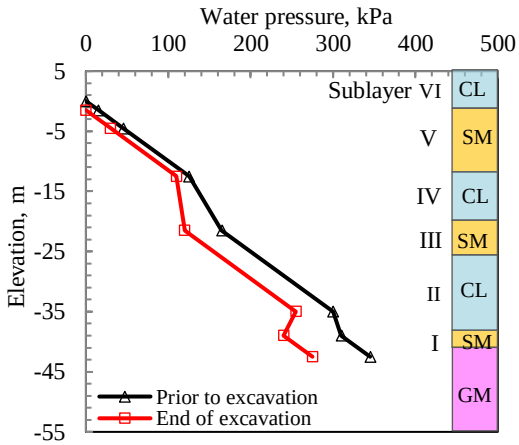


**Figure 4:** Groundwater pressures on the outer face of the diaphragm walls

## 3 Numerical Simulation

Five cases, Case I to Case V, as summarized in Table 1, have been analyzed. Case I is the benchmark case for the verification of the stiffness parameters adopted. Cases II to Case V are conducted for assessing the effects on wall deflections and ground settlements due to variation in excavation widths and in wall thicknesses.

**Table 1:** Cases studied by the HSS model

| Case | Excavation | | Diaphragm wall | | | |
|---|---|---|---|---|---|---|
| | Width B, m | Depth H, m | Thickness t, m | Length L, m | Flexural stiffness $E_cI_c$ , MN-m | Axial stiffness $E_cA_c$ , MN/m |
| I | 11.2 | 23.5 | 0.8 | 31.5 | 750 | 14,056 |
| II | 41.2 | 23.5 | 0.8 | 31.5 | 750 | 14,056 |
| III | 41.2 | 23.5 | 0.7 | 31.5 | 502 | 12,300 |
| IV | 41.2 | 23.5 | 0.6 | 31.5 | 316 | 10,540 |
| V | 41.2 | 14.5 | 2.1 | 31.5 | 13,560 | 36,900 |

### 3.1 Finite Element Mesh

The section analyzed is depicted in Figure 2. The width of the excavation is 11.2 m. Because of symmetry in geometry, only half of the section was analyzed as depicted in Figure 5. The excavation was carried out to a depth of 16.5 m. The lateral extent of the finite element model reaches a distance

Proceedings DOI: 10.21467/proceedings.133
ISBN: 978-81-957605-1-0

Series: AIJR Proceedings
ISSN: 2582-3922

of 140 m from the central axis of the excavation trench. The ground model is 61 m in depth and the diaphragm wall is located at a distance of 5.6 m from the axis of the trench.

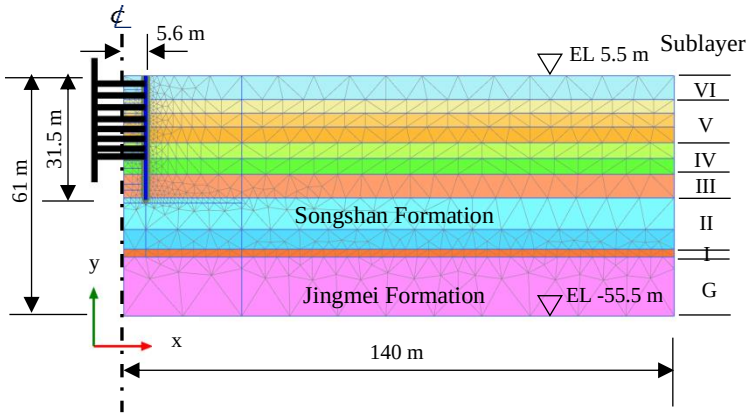


**Figure 5:** Finite element mesh for the analytical section for 9 stages of excavation

### 3.2 Nonlinearity of Soil Behavior - Hardening-Soil With Small-Strain Stiffness Model

The PLAXIS-2D finite element software developed by PLAXIS BV (2013) has become a very popular tool in geotechnical analysis and design. The Hardening-Soil with Small-strain stiffness (HSS) constitutive soil model is an extension of the Hardening-Soil model (Benz 2006, Schanz and Vermeer 1998; Schanz et al. 1999) introduced in the PLAXIS program and is adopted herein to simulate the non-linear stress-strain relationship of soils under loading and unloading. In the HSS model, the parameters adopted to define the hyperbolic stress-strain relationship are as follows:

- $E^{ref}_{50}$ is the reference secant stiffness from standard triaxial test,
- $E^{ref}_{oed}$ is the reference tangent stiffness for oedometer primary loading,
- Erefur is the reference unloading-reloading stiffness,
- m is the exponential factor for stress-level dependency of stiffness,
- $R_f$ is the failure ratio, $R_f = q_a / q_f$ ,
- $q_f$ is the asymptotic value of the shear strength and qa is the failure strength,
- $G^{ref}_0$ is the reference shear modulus at the level of very small strains,
- $\gamma_{0.7}$ is the reference shearing strain to define the behavior of degradation of moduli.

The stress-strain curves can be determined from laboratory tests such as the Ko-consolidated triaxial undrained compression and extension tests. In this study, the stiffness values of soils are related to the undrained shear strengths for clays and the N values for sands. The empirical relationships expressed in Equations 1 to 5 are adopted:

$E^{ref}_{50} = 250\ s_u$ (for clayey soils) **(1)**

$E^{ref}_{50} = 2\ N$ (in MPa for sandy soils) **(2)**

$E^{ref}_{ur} = 5\ E^{ref}_{50}$ **(3)**

$E^{ref}_{oed} = E^{ref}_{50}$ **(4)**

$G^{ref}_0 = 1.2\ E^{ref}_{ur}$ **(5)**

in which $s_u$ is the undrained shear strengths of clayey soils and N is the blow-counts obtained in standard penetration tests for sandy soils. A $\gamma_{0.7}$ value of $0.8 \times 10^{-4}$ is adopted for the various soil layers. The parameters in Equations 1 to 4 have been validated in a previous study by matching the deflection profiles observed in inclinometer SID-6 (Wong and Hwang, 2021). The parameters adopted in this study are summarized in Table 2. The effective shear strength parameters, i.e., the c' and ϕ'values, for the

silty sand strata, are determined from laboratory tests conducted on thin-wall tube specimens. For the clayey layers, c' = $s_u$ and $\phi' = 0^o$ is assumed in the analyses. The dilation angle, $\psi'$, of $2^o$, $0^o$, and $5^o$ are adopted for the sandy, the clayey, and the gravelly soils respectively. The $R_f$ equals 0.9 and an interface reduction factor, $R_{inter}$, of 1 is adopted. The unload-reload Poisson's ratio, $\upsilon_{ur}$, of 0.2 is used as suggested by Benz (2006) and Schanz et al. (1999).

**Table 2:** Soil parameters for the HSS model adopted in the PLAXIS analyses

| Depth m | Soil type | Unit weight $\gamma'$ kN/m$^3$ | N value | Undrained shear strength $s_u$, kPa | Effective cohesion c' kPa | Effective friction angle $\phi'$, deg | Dilation angle $\psi'$ deg | Reference stiffness, MPa | | Initial shear moduli $G^{ref}_0$, MPa |
|---|---|---|---|---|---|---|---|---|---|---|
| | | | | | | | | Secant stiffness $E^{ref}_{50}$ | Unload-reload stiffness $E^{ref}_{ur}$, MPa | |
| 0-6 | CL | 18.8 | 4 | 50 | | | 0 | 12.5 | 63 | 75 |
| 6-17 | SM | 19.2 | 5 | | 0 | 32 | 2 | 10 | 50 | 60 |
| | SM | 19.2 | 8 | | | | 2 | 16 | 80 | 96 |
| | SM | 19.2 | 11 | | | | 2 | 22 | 110 | 132 |
| 17-21 | CL | 18.6 | 6 | 53.7 | | | 0 | 13.4 | 67 | 80.4 |
| 21-25 | CL | 18.6 | 17 | 114.3 | | | 0 | 28.6 | 143 | 170 |
| 25-31 | SM | 19.4 | 18 | | 0 | 32 | 2 | 36 | 180 | 216 |
| 31-39 | CL | 18.9 | | 195.0 | | | 0 | 48.6 | 243 | 290 |
| 39-44 | CL | 18.9 | | 241.0 | | | 0 | 60.2 | 301 | 360 |
| 44-46 | SM | 19.7 | 30 | | 0 | 32 | 2 | 60 | 300 | 360 |
| 46-60 | GM | 19.9 | >100 | | 0 | 40 | 5 | 250 | 1250 | 1500 |

### 3.3 Determination of Small-strain Stiffness

Kung et al. (2009) presented the results of small-strain triaxial tests and bender element tests conducted on undisturbed specimens recovered from clayey Sublayer IV of the Songshan Formation. The specimens were saturated and Ko-consolidated to the in-situ effective stress states. The Ko values applied for consolidation ranged from 0.5 to 0.55. After completing the Ko-consolidation, but prior to the shearing tests, bender element tests were carried out to measure the shear moduli of the clay specimens. Compression and extension undrained triaxial shearing tests were then conducted. The undrained shear strengths profile obtained is consistent with that reported by Hwang et al. (2013) as summarized in Figure 3.

Based on the results of the small-strain triaxial tests and the bender element tests, Kung et al. (2009) obtained $G_{max}/s_u$ ratios ranging from 738 to 788. As defined in Equations 1, 3, and 5, the $G^{ref}_0/s_u$ ratio adopted in this study is 1500. The difference in the maximum shear moduli obtained from bender element tests and back-analysis on field cases could be attributable to the difference in the levels of the strains.

**Table 3:** Strut properties

| Strut level | Depth m | Strut type | Area $A_s$, cm$^2$ | Stiffness $E_sA_s/s$, MN/m | Design preload, kN/m | Strut spacing s, m |
|---|---|---|---|---|---|---|
| S1 | 2.2 | 1H350x350x12x19 | 173.9 | 1,188 | 120 | 3.0 |
| S2 | 5.2 | 1H400x400x13x21 | 218.7 | 1,494 | 250 | |
| S3 | 8.2 | 2H350x350x12x19 | 347.8 | 2,377 | 500 | |
| S4 | 11.0 | 2H350x350x12x19 | 347.8 | 2,377 | 500 | |
| S5 | 14.2 | 2H400x400x13x21 | 437.5 | 2,989 | 553 | |
| S6 to S8 | 16 to 23 | 2H350x350x12x19 | 347.8 | 2,377 | 500 | |

### 3.4 Modeling of the Retaining Structures

The excavation scheme and the retaining structures are depicted in Figure 2. The diaphragm walls are simulated by plate elements and an $E_c$ value of 25,000 MPa is adopted for concrete with a characteristic compressive strength of 28 MPa. The estimated flexural rigidity (denoted as $E_cI_c$ where $I_c$ is the moment

Proceedings DOI: 10.21467/proceedings.133
ISBN: 978-81-957605-1-0

Series: AIJR Proceedings
ISSN: 2582-3922

of inertia) and the axial stiffness (denoted as $E_cA_c$ where $A_c$ is the sectional area) of the diaphragm wall of 0.8 m in thickness are 750 MN-m and 14,056 MN/m respectively. These values have already been reduced from their original values by 30 % to account for tensile cracks and creeping of concrete during excavation.

The excavation was supported by 5 levels of steel struts, i.e., S1 to S5, of which the structural properties are presented in Table 3. The struts are represented by node-to-node anchors. The steel is assumed to be an elastic material with a Young's modulus ($E_s$) of 210 GPa. The preloads in the struts adopted in the analyses were half of those specified in Table 3. To study the effects of excavation depths on wall and ground movements, the excavation was assumed to continue from a depth of 16.5 m further to 23.5 m in 3 stages following the same scheme of excavation adopted in Stage 6 and with the same configuration of the struts.

## 4 Results of Numerical Analysis

### 4.1 Validation of the Methodology and Parameters

The computed wall deflection and surface settlement profiles for Case I are presented in Figure 6. At the final excavation depth of 16.5 m, the computed maximum deflection and toe movements are 33.1 mm and 2.8 mm respectively. The results are compared with the readings of inclinometers SID-6 and SID-7 and with the settlement markers installed along Chongqin South Road in Figure 7. In consideration of the fact that the pit was wider at the locations of both inclinometers, the agreement among the 3 sets of data with Case I is reasonably well. It is noted that the settlement markers were located along Ch.570 m and Ch.584 at distances of 5 m to 9 m to the end wall of Xiaonanmem Station. The over-estimation of the computed results by around 5 mm as shown in Figure 7(b) could be attributable to the presence of this end wall, which restrained the lateral movements of the two walls but is not modelled in the 2-dimensional analysis.

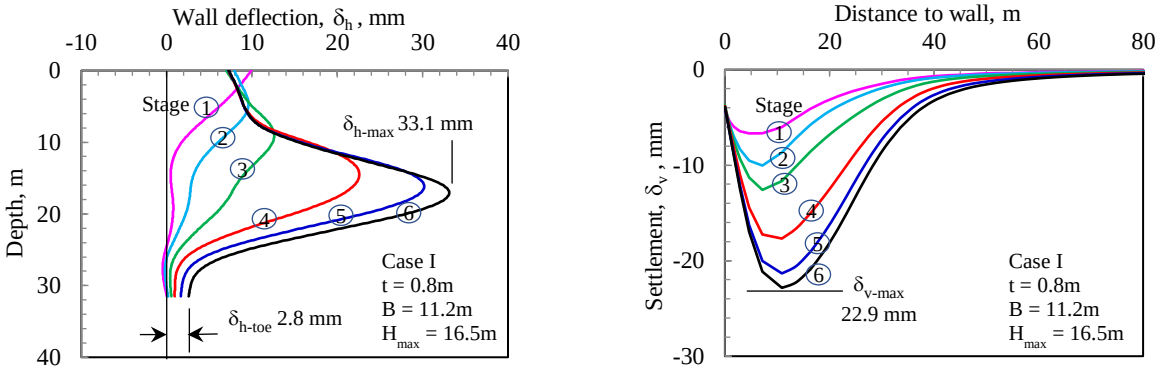


(a) Lateral wall deflections (b) Ground surface settlements

**Figure 6:** Computed wall deflections and surface settlements for Case I

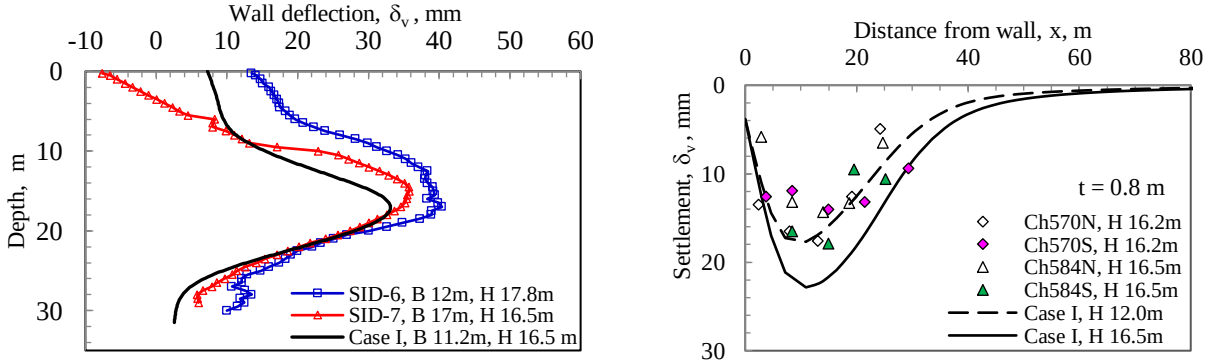


(a) Wall deflections observed in inclinometers (b) Observed surface settlements

**Figure 7:** Comparison between the computed and observed wall deflections and surface settlements for Case I

### 4.2 Effect of the Widths and the Depths of Excavations on Wall Deflections and Ground Settlements

To study the effects of the width of excavation on wall deflections and ground settlements, the excavation is widened from 11.2 m in Case I to 41.2 m in Case II. It can be noted by comparing Figure 8 with Figure 6, the maximum wall deflection increases from 33.1 mm to 45.9 mm in Stage 6 as a result of widening the excavation while the maximum settlement increases from 22.9 mm to 36.3 mm. The maximum wall deflection for Case II would increase from 45.9 mm to 54.6 mm while the ground settlement would increase from 36.3 mm to 48.9 mm, if the excavation were carried out to a depth of 23.5 m.

Figure 9 shows the normalized settlement troughs obtained in Cases I and II. It can be noted that the settlement troughs become wider as the excavation width increases, but the differences among these cases are indeed insignificant for practical purposes.

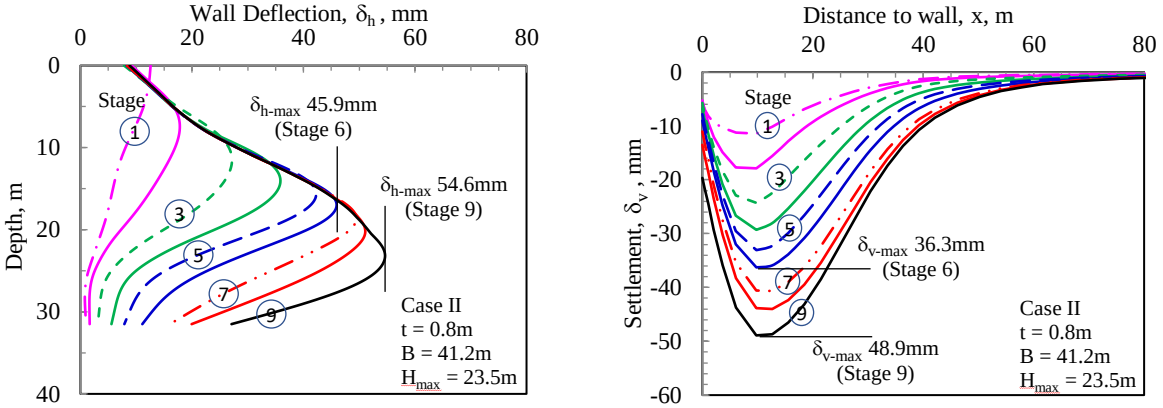


(a) Lateral wall deflections (b) Ground surface settlements

**Figure 8:** Computed wall deflections and surface settlements for Case II

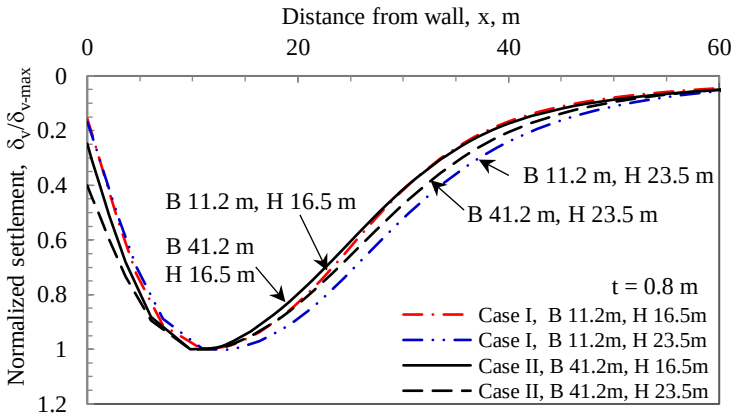


**Figure 9:** Effect of excavation width on the normalized settlement troughs in Case I and Case II

### 4.3 Effect of the Wall Thickness on Wall Deflections and Ground Settlements

Figure 10(a) shows the computed wall deflections profiles obtained in Stage 6 excavation for Cases II, III, and IV. The maximum wall deflection increases from 46.0 mm to 50.2 mm as the wall thickness reduces from 0.8 m to 0.7 m, and to 57.1 mm as the wall thickness reduces further to 0.6 m. The same trend can be noted from Figure 10(b) for Stage 9 excavation. Similarly, Figure 11 shows that the reduction in wall thickness, hence, the stiffness of the wall, does increase ground settlements by, say, roughly 18 %. However, the normalized settlement troughs are hardly affected by wall thickness as depicted in Figure 12.

Proceedings DOI: 10.21467/proceedings.133
ISBN: 978-81-957605-1-0

Series: AIJR Proceedings
ISSN: 2582-3922

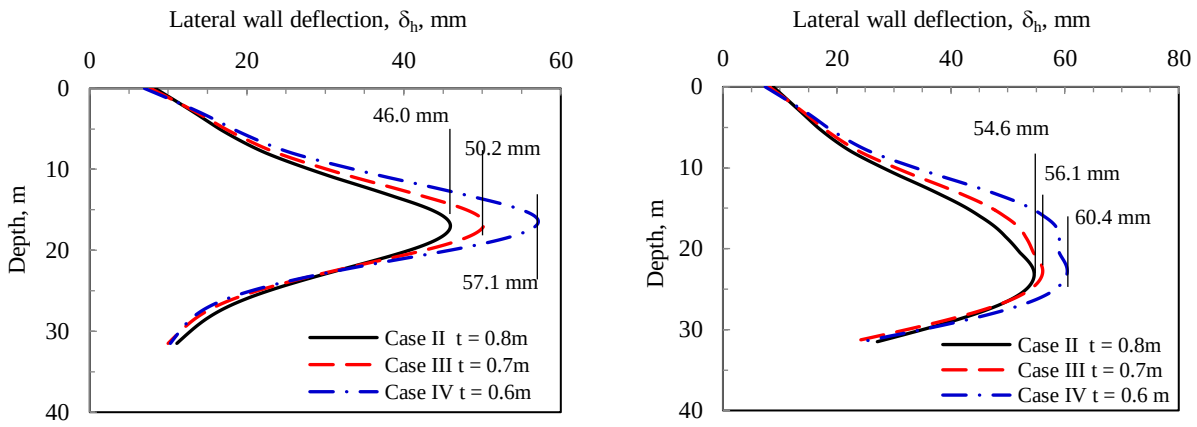


(a) **Stage 6:** Excavated to 16.5 m (b) **Stage 9:** Excavated to 23.5 m

**Figure 10:** Effect of wall thickness – Wall deflections in Cases II, III, and IV

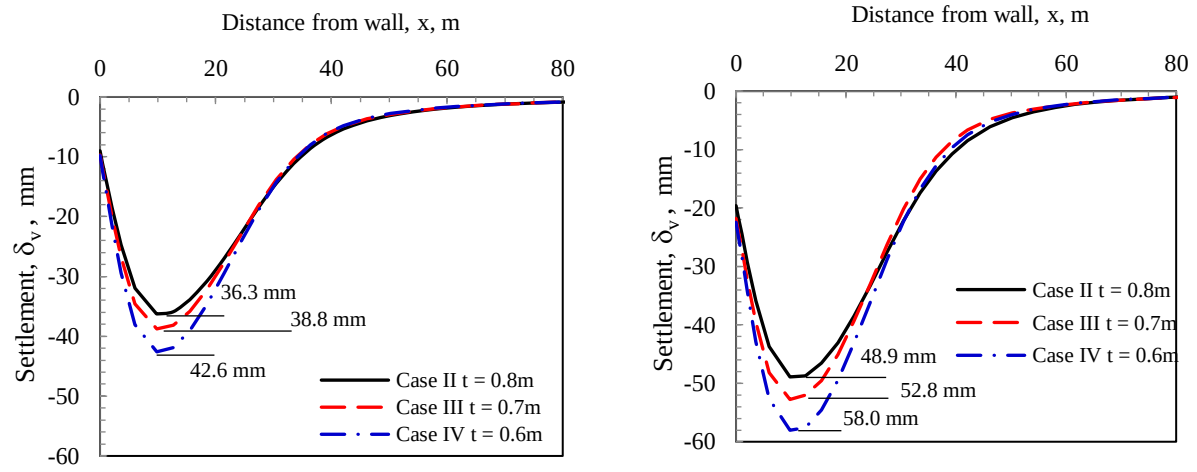


**(a) Stage 6:** Excavated to 16.5 m (b) **Stage 9:** Excavated to 23.5 m

**Figure 11:** Effect of wall thickness – Settlements in Cases II, III and IV

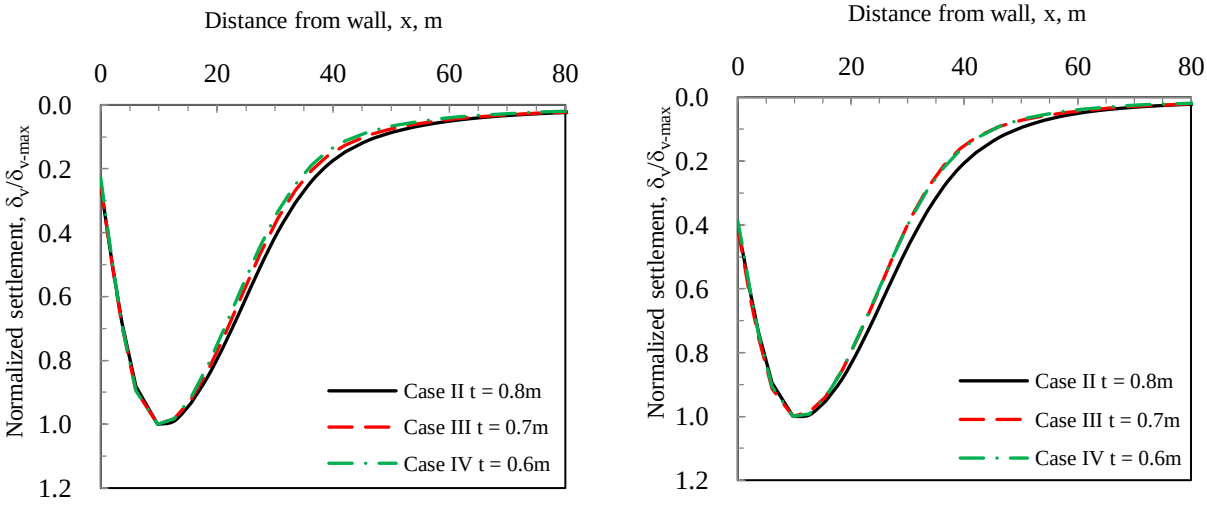


(a) **Stage 6:** Excavated to 16.5 m (b) **Stage 9:** Excavated to 23.5 m

**Figure 12:** Effect of wall thickness – Normalized settlements in Cases II, III and IV

### 4.4 Extent of Influence of Settlements

In addition to the magnitudes of ground settlements, the lateral spreading of the settlements is also an important element in the risk management program for protecting adjacent structures. The extent of the influence of settlements is often correlated to the depth of excavation. Taking Case II as an example, Figure 13(a) shows the settlement troughs in all the 9 stages of excavation with the settlements, $\delta_v$, normalized by the maximum settlement, $\delta_{v\text{-}max}$, and the distance from the wall, x, normalized by the depth of excavation, H.

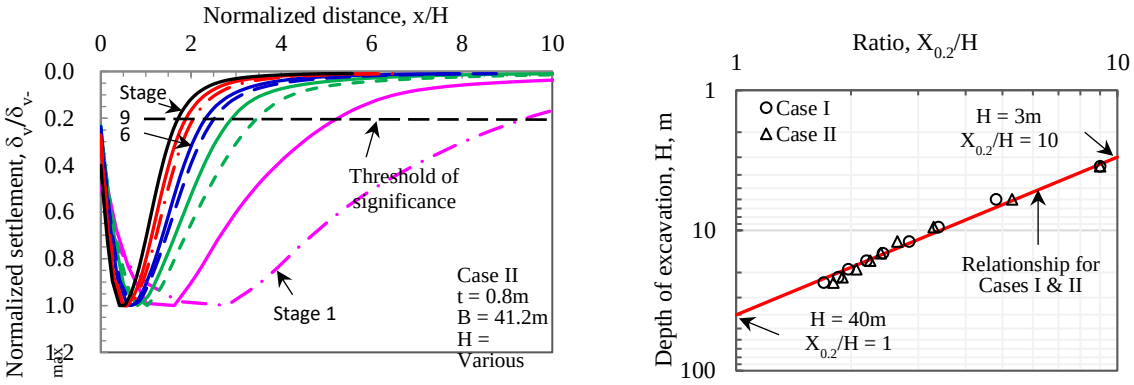


(a) Normalized settlement troughs (b) Width of settlement trough

**Figure 13:** Estimation of significant ground settlements

The normalized settlement troughs would become narrower and narrower as the depths of excavation increase. If 20 % is adopted to be the threshold for significance, the $X_{0.2}/H$ ratio, in which $X_{0.2}$ is the distance from the wall to where the settlement equals 20 % of the maximum settlement, can be related to the depth of excavation as depicted in Figure 13(b). The regression function can be defined in a log-log scale by two control points, at H values of 3 m and 40 m. For the excavation depths H of 3 m and 40 m, the normalized distance to the wall, i.e., the $X_{0.2}/H$ ratios, are 10 and 1 respectively. It appears that this relationship is not sensitive to the excavation widths and is expected to be applicable in general cases. Based on Figure 13(a), it is recommended to assume ground settlements drop linearly to zero at a distance of 10H for excavations shallower than 10 m in depth and 5H for deeper excavations. The proposed empirical relationship is verified by field observations and results of the centrifuge test shown in Section 5.3. It should however be noted that the results of the analyses presented are performed with consideration given only to the equilibrium of stresses induced in soils as the excavation proceeds and the balances of forces acting on the wall and struts. Consolidation settlements are not accounted for.

## 5 Comparison with Field Observations

To verify the applicability of the results of the analyses, the computed wall deflections and ground settlements are compared with the field observations and the centrifuge tests reported in Wong & Patron (1993), Hsieh & Ou (1998), Panchal et al. (2017) and Panchal et al. (2018) as follows.

### 5.1 Cases Reported in Wong and Patron (1993)

Wong and Patron (1993) reported the wall deflections and ground settlements caused by excavation in 8 cases in the T2 Zone of the Taipei Basin. As summarized in Table 4, the excavation widths for these cases range from 35 m to 61 m and the final excavation depths range from 11.1 m to 21.7 m. The diaphragm walls were 0.7 m and 0.6 m in thickness. The majority of the wall lengths are 60 % to 80 % of the length of 31.5 m adopted in the analysis. The wall deflections for the wall thicknesses of 0.7 m

Proceedings DOI: 10.21467/proceedings.133
ISBN: 978-81-957605-1-0

Series: AIJR Proceedings
ISSN: 2582-3922

and 0.6 m are compared with those computed in Case III and Case IV in Figure 14 and Figure 15 respectively.

**Table 4:** Summary of excavation cases in T2 Zone presented by Wong & Patron (1993)

| Case | Wall dimension, m | | Excavation geometry, m | | H/L | Strut levels | Excavation case |
|---|---|---|---|---|---|---|---|
| | Thickness, t | Length, L | Depth, H | Width, B | | | |
| A1 | 0.7 | 21 | 16.2 | 61 | 0.77 | 4 | Taiwan Power |
| A4 | | 27 | 14.7 | 37 | 0.54 | 5 | Chun Wei |
| A7 | | 34 | 21.7 | 46 | 0.64 | 7 | Cathay Life |
| A8 | | 30 | 17.1 | 40 | 0.57 | 5 | China Times |
| A2 | 0.6 | 17 | 11.1 | 52 | 0.65 | 3 | Kuan Min |
| A3 | | 23 | 11.4 | 35 | 0.50 | 3 | Central Insurance |
| A5 | | 25 | 12.3 | 37 | 0.49 | 4 | Chung Yang Pa Shi |
| A6 | | 22 | 12.6 | 48 | 0.57 | 4 | Shin-I |

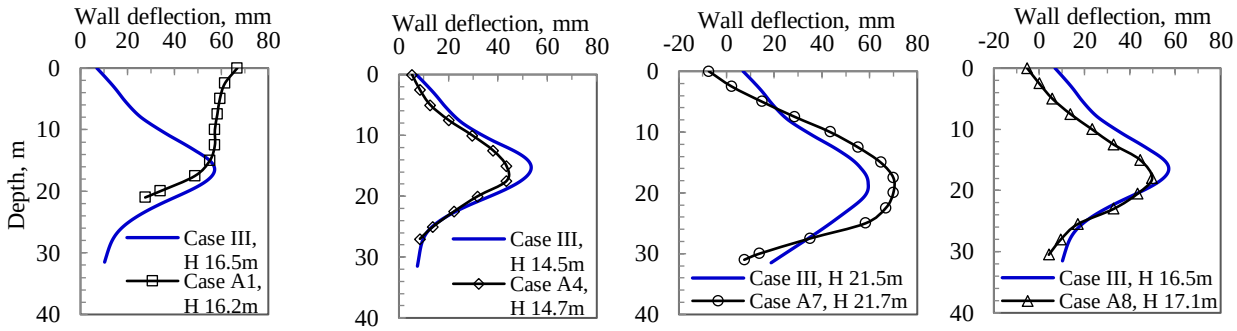


(a) A1: Taiwan Powe (b) A4: Chun Wei (c) A7: Cathay Life (d) A8: China Times

**Figure 14:** Computed wall deflections in the final excavation stage for cases with a wall thickness 0.7 m

As can be noted from Figure 14(a), the large deflections that occurred in Case A1 could probably be due to the short wall length of 21 m, which is 70 % of the length of 31.5 m adopted in the analysis. Other than that, despite the various uncertainties associated with the field operations, such as preloading and over-excavation, the computed wall deflection profiles are reasonably close to those observed.

The settlement profiles for the eight cases are presented in Figure 16. Comparing with those computed profiles in Case III and Case IV at the excavation depths of 16.5 m and 14.5 m respectively, the observed and the computed settlement profiles are reasonably close. Based on Figures 14 to 16, it is concluded that the HSS soil model could reliably estimate the wall deflections and ground settlements simultaneously.

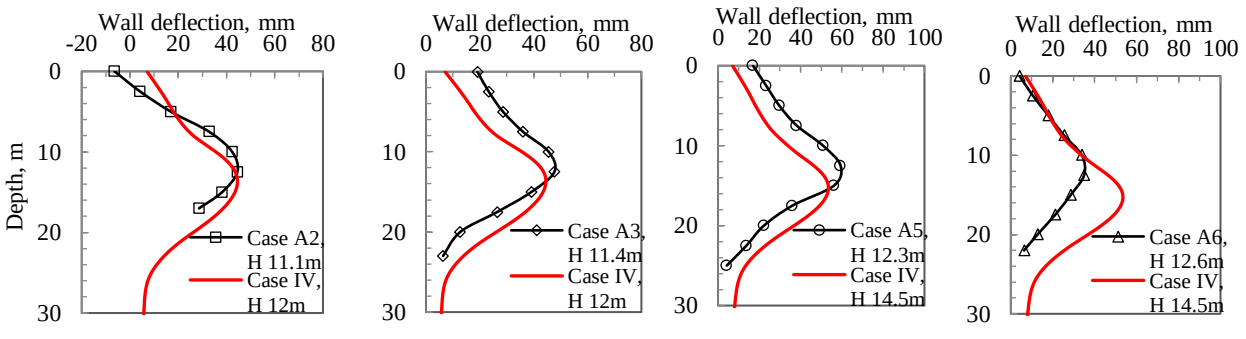


(a) A2: Kuan Min (b) A3: Central Insurance (c) A5: Chung Yang Pa Shi (d) A6: Shin I

**Figure 15:** Computed wall deflections in the final excavation stage for cases with a wall thickness of 0.6 m

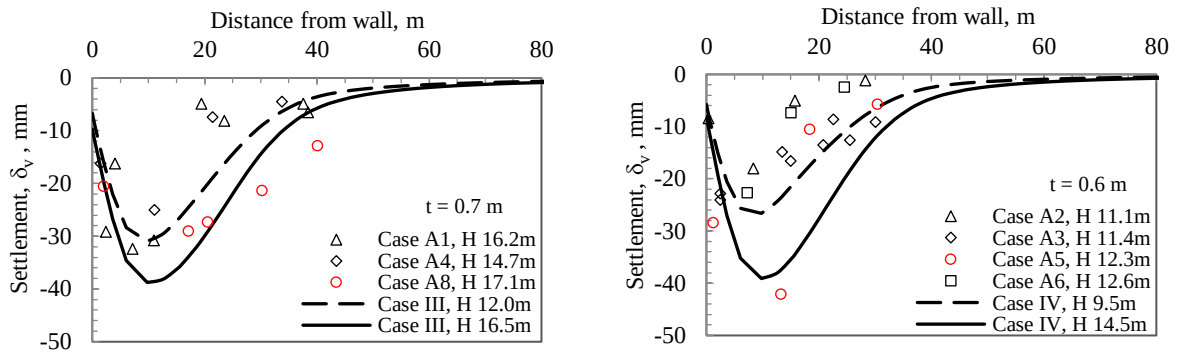


(a) Wall thickness 0.7 m (b) Wall thickness 0.6 m

**Figure 16:** Computed settlements in the final excavation stage for the cases reported in Wong & Patron (1993)

## 5.2 Cases Reported in Hsieh and Ou (1998)

Hsieh and Ou (1998) collected 7 excavation cases in soft ground located in Taipei, London, Chicago, Oslo, and in Japan. The final excavation depths ranged from 11 m to 20 m as summarized in Table 5. Among these 7 cases, Cases B1 and B3 to B4 were supported with floating walls with the toe levels at 10 m to 15 m above the competent strata. The walls for other cases, Cases B2, B6, and B7, were end bearing walls with the toes founded on bedrock or on the gravel stratum.

**Table 5:** Summary of excavation cases studied by Hsieh & Ou (1998)

| Case | Wall dimension, m | | Excavation geometry, m | | H/L | Strut levels | Location |
|---|---|---|---|---|---|---|---|
| | Thickness, t | Length, L | Depth, H | Width, B | | | |
| B1 | Diaphragm wall 0.9m | 35 | 19.7 | 41 | 0.56 | 6 | Taipei, TNEC |
| B2 | Diaphragm wall | 31 | 18.5 | 35 | 0.60 | 6 | Taipei |
| B3 | Steel concrete wall | 32 | 17.0 | 30 | 0.53 | 5 | Japan |
| B4 | Diaphragm wall | 30 | 18.5 | 50 | 0.62 | 5 | London |
| B5 | Steel sheet pile | 19.2 | 12.2 | 12.2 | 0.64 | 4 | Chicago |
| B6 | Steel sheet pile | 16 | 11.0 | 11 | 0.69 | 5 | Oslo |
| B7 | Diaphragm wall | 33 | 20.0 | 70 | 0.61 | 5 | Taipei, Far East Enterprise |

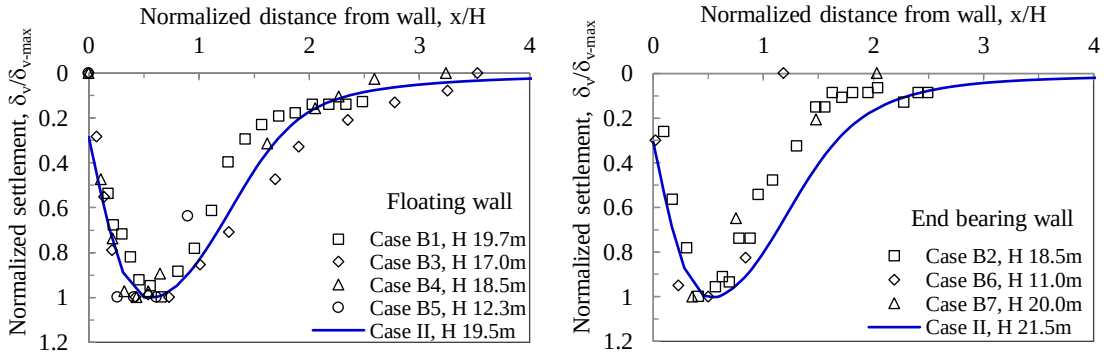


(a) Floating walls (b) End bearing walls

**Figure 17:** Computed settlements in the final excavation stage for the cases reported in Hsieh & Ou (1998)

The computed settlement profiles are compared with the settlements obtained in Case II (H = 19.5 m for Stage 7 and H = 21.5 m for Stage 8) in Figure 17. The normalized settlement profiles are reasonably close to the observed profiles.

Proceedings DOI: 10.21467/proceedings.133
ISBN: 978-81-957605-1-0

Series: AIJR Proceedings
ISSN: 2582-3922

### 5.3 Centrifuge Tests by Panchal et al. (2017; 2018)

Ground movements associated with excavations are a complex combination of lateral and vertical wall movements, wall bending, and ground heave. Centrifuge modeling allows researchers to simply and physically simulate complex geotechnical problems, especially on nonlinear geotechnical materials. Panchal et al. (2017; 2018) reported the results of 3 centrifuge modeling tests, as summarized in Table 6, on an underwater excavation case to study the relationship between the ground movements and basal heave below the final excavation level. The model comprised half an excavation, 150 mm wide and 75 mm deep, representing 24 m and 12 m at prototype scale, respectively. The toe of the retaining wall was embedded 55 mm into the clay, equating to 8.8 m at prototype scale, giving a total length of 20.8 m of the wall.

To confirm whether the normalized settlement troughs obtained by numerical analyses are applicable to centrifuge tests, Case V, referring to Table 1, was conducted and the results are compared with those reported by Panchal et al. (2017; 2018) in Figure 18. The agreement between these 2 sets of data is very encouraging.

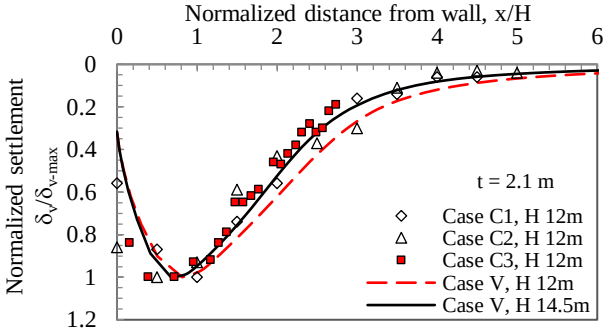


**Figure 18:** Comparison of settlements computed in Case V and those reported in Panchal et al. (2017 & 2018)

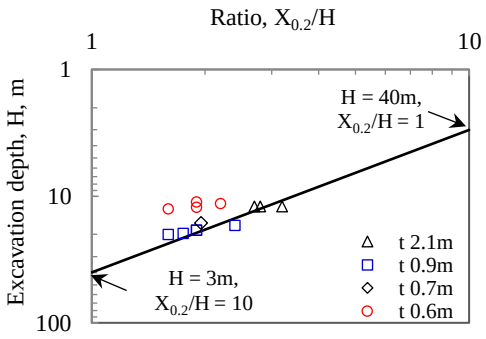


**Figure 19:** Width of settlement trough at 20% of maximum settlement for various case histories

**Table 6:** Summary of centrifuge models reported by Panchal et al. (2017; 2018)

| Case | Wall dimension, m | | Excavation geometry, m | | Main feature | Reference |
|---|---|---|---|---|---|---|
| | Thickness, t | Length, L | Depth, H | Width, B | | |
| C1 | 2.1 | 20.8 | 12 | 48 | Underwater excavation | Panchal et al. (2017) |
| C2 | 2.1 | 20.8 | 12 | 48 | Reference test | Panchal et al. (2018) |
| C3 | 2.1 | 20.8 | 12 | 48 | Lime stabilized | |

As can be noted from Figure 19, the $X_{0.2}/H$ ratios obtained in various case histories and centrifuge tests fit very well with the relationship established based on the results obtained in all other cases. The empirical relationship between the widths of the settlement trough and the excavation depths has thus been verified.

## 6 Conclusions

Parametric studies on a typical excavation case in soft ground supported by diaphragm walls using 2-Dimensional finite element analysis have been conducted. Various excavation widths, wall thicknesses and excavation depths have been adopted. The following conclusions could be drawn:

(1) The nonlinear Hardening-Soil with small-strain stiffness constitutive soil model could reliably estimate the wall deflections and ground settlement simultaneously in the numerical analysis.

(2) There is the trend of the larger the excavation depth, the narrower the width of the settlement trough.

(3) The shapes of the normalized settlement profiles are primarily affected by the depths of excavations and are relatively insensitive to the width of excavation or to the thickness of the retaining wall.

(4) An empirical relationship between the widths of the settlement trough and the excavation depths has been established for assessing the influence of surface settlements.

As the computed distribution of the settlement troughs and the magnitude of the settlements have agreed with those observed in the field, the stiffness parameters adopted for the Hardening-soil with the small-strain stiffness model have been validated.

## 7 Publisher's Note

AIJR remains neutral with regard to jurisdictional claims in published maps and institutional affiliations.

## References

Benz, T. (2006). Small-strain stiffness of soils and its numerical consequence. Dissertation of thesis, the Institute of Geotechnics, University Stuttgart.

Chin, C. T., Crooks, A. J. H. and Moh, Z. C. (1994). Geotechnical properties of the cohesive Sungshan deposits. Geotechnical Engineering, J. Southeast Asian Geotechnical Society, Taipei, Taiwan 25(2), 77-103. (in Chinese)

Chin, C. T. and Liu, C-C. (1997). Volumetric and undrained behaviors of Taipei silty clay. J. Chinese Institute of Civil and Hydraulic Engineering, Taipei, Taiwan 9(4), 665-678. (in Chinese)

Hsieh, P.G. and Ou, C.Y. (1998). Shape of ground surface settlement profiles caused by excavation. Canadian Geotechnical Journal 35(6), 1004-1017.

Hwang, R., Moh, Z. C. and Hu, I-C. (2013). Effects of consolidation and specimen disturbance on strengths of Taipei Clays, Geotechnical Engineering, J. of SEAGS & AGSSEA, March, Bangkok, 44(1), 9-18.

Kung, G.T.C, Ou, C.Y. and Juang C.H. (2009). Modelling small-strain behavior of Taipei clays for finite element analysis of braced excavations. Computers and Geotechnics 36 (2009), 304-319

MAA (1987) Engineering properties of the soil deposits in the Taipei Basin, Report No. 85043, Ret-Ser Engineering Agency and Taipei Public Works Department, Taipei (in Chinese)

Moh, Z. C. and Ou C. D. (1979). Engineering characteristics of Taipei Silt. Proc., 6th Asian Regional Conference on Soil Mechanics and Foundation Engineering, Singapore, 1, 155-158.

Panchal, J.P., McNamara, A.M. and Stallebrass, S.E. (2017). Minimising base heave from deep excavations in soft soil conditions using underwater construction methods. Proceedings of the 19th International Conference on soil mechanics and Geotechnical Engineering, Seoul, Korea, 3019-3022.

Panchal, J.P., McNamara, A.M. and Stallebrass, S.E. (2018) Physical modelling of lime stabilization in soft soils around deep excavations, The Journal of Deep Foundations Institute, Volume 11, 137-147

PLAXIS, B. V. (2013). PLAXIS reference manual. Plaxis BV, Delft, the Netherlands.

Schanz, T. and Vermeer, P. A. (1998). On the Stiffness of Sands. Pre-failure Deformation Behaviour of Geomaterials, ICE, London, UK, 1998.

Schanz, T., Vermeer, P.A. and Bonnier, P.G. (1999). The hardening soil model: formulation and verification. Beyond 2000 in Computational Geotechnics. Rotterdam, the Netherlands, 281-290.

Wong, L. W. and Hwang, R. N. (2021). Effectiveness of cross-walls in reducing wall deflections in deep excavations. Proceedings, 41st HKIE Geotechnical Division Annual Seminar, Hong Kong 18 May 2021, 282-295.

Wong, L.W. and Patron B.C. (1993). Settlements induced by deep excavations in Taipei. Proceedings of the 11th Southeast Asian Geotechnical Conference, Singapore, 787~791.

Proceedings DOI: 10.21467/proceedings.133
ISBN: 978-81-957605-1-0

Series: AIJR Proceedings
ISSN: 2582-3922